

## Measurement of the spectrum of resonance fluorescence from a two-level atom in an intense monochromatic field\*

R. E. Grove, F. Y. Wu, and S. Ezekiel

*Research Laboratory of Electronics, Massachusetts Institute of Technology, Cambridge, Massachusetts 02139*

(Received 24 May 1976; revised manuscript received 12 August 1976)

We have made measurements of the spectrum of resonance fluorescence emitted by sodium atoms in an intense, uniform, monochromatic field. The transition used in the experiment was between the  $3^2S_{1/2}$  ( $F = 2, m_F = 2$ ) ground state and the  $3^2P_{3/2}$  ( $F' = 3, m_{F'} = 3$ ) excited state. A separate light beam, circularly polarized and resonant with this transition, was used to prepare the sodium atoms in the  $F = 2, m_F = 2$  magnetic sublevel. This pumping scheme was used to obtain the spectrum for both on- and off-resonance excitations. The measurements are in good agreement with Mollow's calculation. In addition, we describe conditions under which we observed asymmetric spectra similar to those of earlier experiments.

### INTRODUCTION

The spectrum of resonance fluorescence is of fundamental importance to the understanding of the interaction of radiation with matter. Recently there have been a number of theoretical treatments<sup>1-18</sup> and a few experimental studies<sup>19-22</sup> of this problem.

Most of the theoretical work deals with the ideal system of an atom with only two energy levels. Earlier observations of the spectrum were difficult to interpret because of the lack of a true two-level system. In this paper we present high-resolution measurements of the spectrum of resonance fluorescence from a carefully prepared two-level atom. For the first time, experimental spectra are quantitatively compared with theory for both on- and off-resonance excitations. In addition, we include data which may aid in the explanation of

the conflicting results of earlier experiments regarding the symmetry of the spectrum.<sup>19-22</sup>

### THEORETICAL PREDICTIONS

Weisskopf<sup>23</sup> first showed that if a two-level atom is excited by weak, monochromatic, resonant radiation, the resulting fluorescence is also monochromatic and of the same frequency as the incident light. The case of strong-field excitation, in which the induced transition rate is comparable to, or greater than the spontaneous emission rate, has been studied only recently, and with conflicting results. A variety of spectral distributions have been predicted,<sup>1-18</sup> most of them consisting of three peaks. The spectrum which is now generally accepted was first calculated by Mollow<sup>5</sup> using a *c*-number driving field and some statistical assumptions. It is given [from Ref. 5, Eqs. (4.15) and (3.23)] by

$$g(\nu) = \frac{8\pi\bar{n}_\infty^2 \left[ \frac{1}{4}\Gamma^2 + (\Delta\nu)^2 \right]}{\Omega^2} \delta(\nu - \nu_L) + \Gamma\bar{n}_\infty\Omega^2 \frac{(\nu - \nu_L)^2 + \frac{1}{2}\Omega^2 + \Gamma^2}{\Gamma^2 \left[ \Omega^2/4\bar{n}_\infty - 2(\nu - \nu_L)^2 \right]^2 + (\nu - \nu_L)^2 \left[ \Omega^2 + (\Delta\nu)^2 + \frac{5}{4}\Gamma^2 - (\nu - \nu_L)^2 \right]^2}, \quad (1)$$

where  $\Omega = \mu E/\hbar$ ;  $E$  is the electric field strength;  $\mu$  is the electric dipole matrix element;  $\Gamma$  is the natural width of the transition;  $\nu_L$  is the frequency of the incident radiation;  $\Delta\nu = \nu_L - \nu_0$ , where  $\nu_0$  is the transition resonance frequency, and

$$\bar{n}_\infty = \frac{\frac{1}{4}\Omega^2}{\frac{1}{2}\Omega^2 + (\Delta\nu)^2 + \frac{1}{4}\Gamma^2}. \quad (2)$$

Figures 6(a)–6(c) are theoretical plots of  $g(\nu)$  for both on- and off-resonance excitation, corresponding to  $\Delta\nu = -50$  MHz, 0, and +50 MHz respectively, with  $\Gamma = 10$  MHz and  $\Omega = 78$  MHz. The spectrum consists of a  $\delta$  function elastic component and a three-peaked inelastic component. The elastic part is dominant in weak fields but negligible under strong, resonant excitation.

In the limit of very intense fields ( $\Omega \gg \Gamma$  and  $\Omega \gg \Delta\nu$ ) the spectrum reduces to

$$g(\nu) = 2\pi \frac{(\Delta\nu)^2 + \frac{1}{4}\Gamma^2}{\Omega^2} \delta(\nu - \nu_L) + \frac{\frac{3}{16}\Gamma}{(\nu - \nu_L + \Omega)^2 + \frac{9}{16}\Gamma^2} + \frac{\frac{1}{4}\Gamma}{(\nu - \nu_L)^2 + \frac{1}{4}\Gamma^2} + \frac{\frac{3}{16}\Gamma}{(\nu - \nu_L - \Omega)^2 + \frac{9}{16}\Gamma^2}. \quad (3)$$

In this limit, the inelastic component clearly has the form of three Lorentzians with heights in the ratio 1:3:1 and widths of  $\frac{3}{2}\Gamma$ ,  $\Gamma$ , and  $\frac{3}{2}\Gamma$ . The separation between central and side peaks is the Rabi frequency  $\Omega' = [\Omega^2 + (\Delta\nu)^2]^{1/2}$ .

The spectrum has now been derived using fully quantum-mechanical treatments and without any statistical assumptions.<sup>16,17,18</sup> Cohen-Tannoudji<sup>15</sup>

has also presented a clear physical interpretation of the three-peaked spectrum.

#### EARLIER EXPERIMENTAL RESULTS

The first observation of the three-peaked strong-field spectrum was reported by Schuda, Stroud, and Hercher.<sup>19</sup> In their experiment, a linearly polarized cw dye-laser beam intersected a sodium atomic beam at right angles, and excited the  $3^2S_{1/2}(F=2)$ - $3^2P_{3/2}(F'=3)$  transition. The fluorescence was analyzed by a Fabry-Perot interferometer along a mutually orthogonal direction. Subsequent experiments,<sup>20,21</sup> which used essentially the same arrangement, yielded spectra with improved resolution. However, a quantitative comparison with theoretical predictions was not possible because a two-level atom was not used. In a more recent work, Walther<sup>22</sup> obtained improved on-resonance spectra by using circularly polarized light.

The weak-field spectrum has also been observed by several groups<sup>21,22,24,25</sup>; the fluorescence linewidth was shown to be less than the natural width.

#### PREPARATION OF A TWO-LEVEL SYSTEM

Quantitative comparison with theory requires that the incident radiation interact with atoms that can make transitions between only two states. The  $3^2S_{1/2}(F=2)$  and  $3^2P_{3/2}(F'=3)$  states in sodium are a potential two-level system because the upper state  $F'=3$  can decay only to the  $F=2$  state. However, both hyperfine levels consist of degenerate magnetic sublevels with unequal electric dipole matrix elements ( $\mu$ ) connecting them. Figure 1 shows the sublevels and the relative magnitudes of the matrix elements.

Application of intense, resonant, linearly ( $\pi$ ) polarized light induces  $\Delta m=0$  transitions between the  $F=2$  and  $F'=3$  states. There are five such transitions, and since they have different Rabi

frequencies, the side peaks of the fluorescence spectrum would therefore be broadened. However, the broadening is not as severe as might be expected because most of the  $F=2(m_F=\pm 2)$  atoms are pumped to other sublevels ( $m_F=-1, 0, +1$ ) soon after they enter the intense field. Another problem is the pumping of  $F=2$  ground-state atoms to the  $F=1$  ground state via the nearly resonant ( $F=2$ )-( $F'=2$ ) transition. Since the  $F=1$  atoms are not excited by the incident radiation, this process depletes the population available for resonant interaction. This depletion becomes severe when the laser is tuned near the ( $F=2$ )-( $F'=2$ ) transition frequency, just 60 MHz below ( $F=2$ )-( $F'=3$ ).

The above difficulties may be overcome by using circularly polarized light.<sup>26,22</sup> Intense  $\sigma^+$  circularly polarized light induces  $\Delta m=+1$  transitions (marked with arrows in Fig. 1), and thereby pumps most of the  $F=2$  atoms into the  $m_F=2$  sublevel. From this sublevel, the only allowed  $\Delta m=+1$  transition is to the  $F'=3(m_F=3)$  level. The nonresonant transitions  $F=2(m_F=2)$ - $F'=2(m_F'=-2, -1, 0, +1, +2)$  are also forbidden in the electric dipole approximation. Thus, the  $F=2(m_F=2)$  atoms may be considered a two-level system. The effect of the atoms in the  $F=1$  ground state is negligible because of the large separation (1772 MHz) between the  $F=1$  and  $F=2$  levels.

Optical pumping with  $\sigma^+$  light is completed quickly only if the incident light is moderately intense and resonant with the ( $F=2$ )-( $F'=3$ ) line. With off-resonance excitation, optical pumping is much slower, and a true two-level system cannot be obtained without a large increase in laser intensity or interaction time. This difficulty may be avoided by using a resonant "pump" beam to prepare the atoms before they reach the interaction region.

Figure 2 shows the experimental arrangement we used to demonstrate the preparation of sodium as a two-level system. The output of a single-fre-

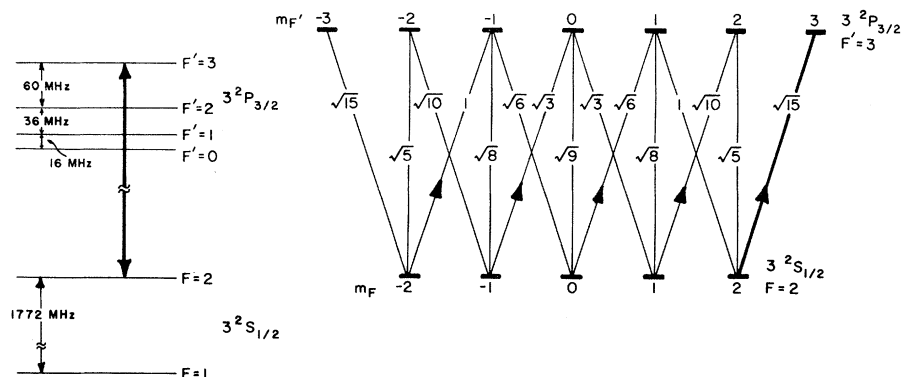


FIG. 1. Energy-level diagram of sodium  $D_2$  line hyperfine structure and the degenerate magnetic sublevels involved in ( $F=2$ )-( $F'=3$ ) transitions. Relative values of the electric dipole matrix elements  $\mu$  are given for each transition.

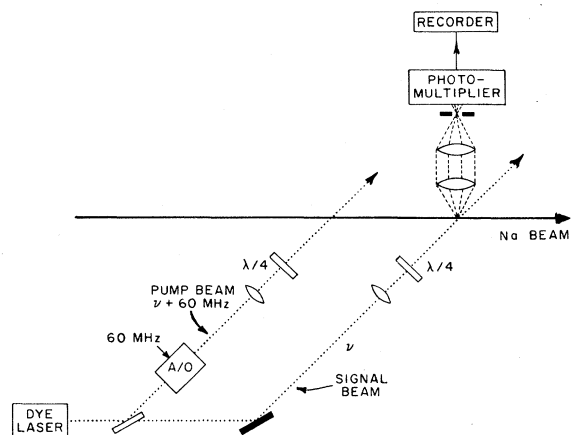


FIG. 2. Experimental setup for demonstrating the preparation of a two-level system.

quency cw dye laser is split into parallel "pump" and "signal" beams, which are separated by 1.2 cm and intersect a sodium atomic beam at right angles. The pump beam is shifted 60 MHz (the separation between the  $F' = 2$  and  $F' = 3$  states) above the signal-beam frequency by an acousto-optic (A/O) shifter. The pump beam intensity is  $30 \text{ mW/cm}^2$  while the signal beam is attenuated to  $1 \text{ mW/cm}^2$ . Each beam is better than 97%  $\sigma^+$  circularly polarized by a quarter-wave plate.

We monitored the fluorescence intensity induced by the weak signal beam as the laser frequency was scanned over the  $(F = 2)-(F' = 1, 2, 3)$  transi-

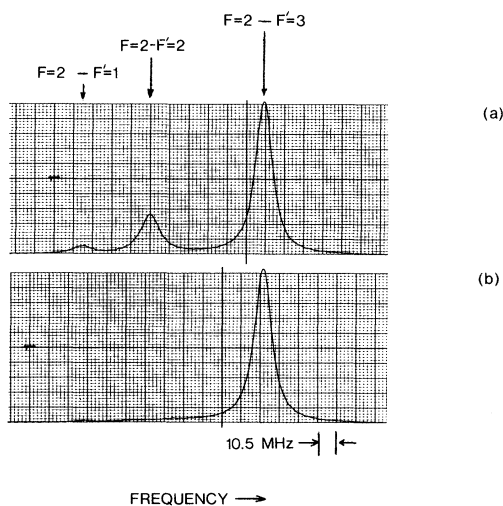


FIG. 3. Demonstration of the preparation of sodium as a two-level system, showing the effect of optical pumping on hyperfine absorption spectrum. (a) Without pump beam. (b) With pump beam. 10.5 MHz/large division; scan rate 50 MHz/sec.

tions. Due to the 60-MHz separation between the pump- and signal-beam frequencies, resonance of the signal beam with the  $(F = 2)-(F' = 2)$  transition coincided with resonance of the pump beam with the  $(F = 2)-(F' = 3)$  transition. When the pump beam was blocked, the fluorescence associated with the three transitions was observed [Fig. 3(a)]. When the laser was scanned with the pump beam unblocked, as shown in Fig. 3(b), the  $(F = 2)-(F' = 2)$  line disappeared, indicating that no  $(F = 2)-(F' = 2)$  absorption occurred. The pump beam had depopulated those states ( $F = 2, m_F = -2, -1, 0, +1$ ) from which  $\Delta m = +1$  transitions to the  $F' = 2$  state are allowed. In other words, the pump beam had transferred most of the  $F = 2$  atoms into the  $m_F = 2$  sublevel. Figure 3(b) shows that the  $(F = 2)-(F' = 1)$  line was also attenuated because of off-resonance pumping.

To prevent redistribution of the sublevel populations by stray fields in the region between laser beams, it was necessary to apply a weak magnetic field (0.7 G) parallel to the laser beams.

#### EXPERIMENTAL APPARATUS

Figure 4 outlines the setup used both to prepare sodium as a two-level system and to measure the fluorescence spectrum. The dye laser is similar to the one described elsewhere.<sup>27</sup> It produces up to 40 mW of single-frequency power at 5890 Å. The laser is both frequency and intensity stabilized such that the spectral width is less than 250 kHz and intensity fluctuations are less than 2%.

The sodium is heated in an oven at temperatures up to  $530^\circ\text{C}$  and is collimated by two 0.5-mm-diam apertures separated by 40 cm. The sodium beam orthogonally intersects the laser beams 20 cm

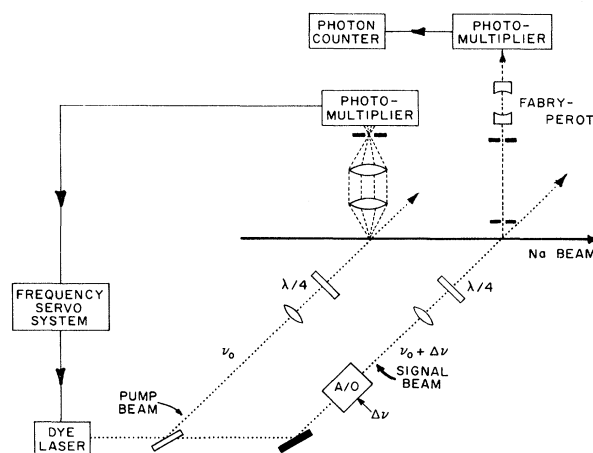


FIG. 4. Experimental setup used to measure the spectrum of resonance fluorescence. The A/O shifter is removed to obtain on-resonance data.

after the second aperture. Fluorescence induced by the pump beam is monitored for long-term laser frequency stabilization.<sup>27</sup>

Much attention was given to the uniformity of the laser intensity in the signal-beam interaction region. Both laser beams have Gaussian profiles with distances between  $1/e^2$  points of 2.4 mm in the horizontal direction (along the atomic beam) and 2.9 mm in the vertical direction. To measure the beam profile at the interaction region, the beam was directed onto a 100- $\mu\text{m}$  pinhole at an equivalent distance from the laser. The pinhole was translated, and the transmitted light detected by a photodiode. The measured intensity profile along the horizontal direction is compared with a Gaussian in Fig. 5.

The fluorescence emitted from the central part of the signal-beam interaction region is collimated by two 0.5-mm-diam apertures placed 4 and 40 cm above the interaction region. The collimated fluorescence is analyzed by a thermally insulated Fabry-Perot interferometer with a 2-MHz instrument width. Under these conditions, most of the observed fluorescence is emitted by atoms in a laser electric field that is within 4% of the peak value.

The light transmitted by the Fabry-Perot interferometer is detected by a cooled photomultiplier, followed by photon-counting electronics. The data are recorded on magnetic tape for subsequent averaging and filtering.

At an oven temperature of 530°C, the expected flux through the 0.5-mm source aperture is  $9 \times 10^{18}$  atoms/sec. The resulting beam density at the interaction region is  $6 \times 10^9$  atoms/cm<sup>3</sup>, corresponding to  $9 \times 10^5$  atoms in the volume under observation. The mean distance between atoms is 6  $\mu\text{m}$ , and the average velocity is  $1 \times 10^5$  cm/sec. When the atoms are excited by strong, resonant

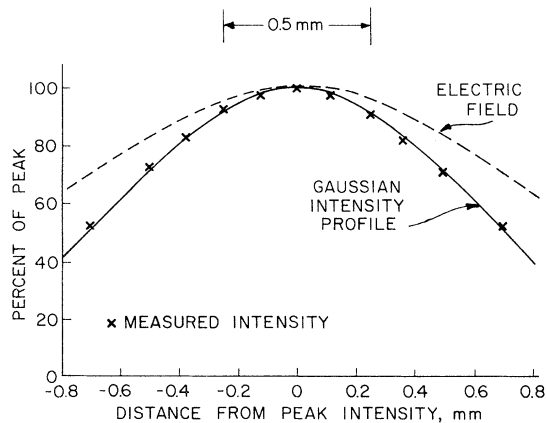


FIG. 5. Intensity profile of laser beams (horizontal direction).

radiation ( $\Omega \gg \Gamma$ ), they spend almost half their time in the upper state; thus the mean spontaneous emission rate per atom is  $\frac{1}{2}\Gamma$ . Allowing for the fact that only  $\frac{5}{8}$  of the atoms are initially in the  $F=2$  ground state and assuming that pumping to  $F=1$  is negligible, we expect about  $2 \times 10^{13}$  photons/sec emitted in all directions. The collimation angle of 1.3 mrad reduces this to  $2 \times 10^6$  photons/sec entering the Fabry-Perot interferometer.

At the high oven temperature of 530°C, the actual Doppler width of the atomic beam is greater than the width calculated from the aperture geometry. This is caused by collisions at the primary aperture, which increase the effective size of the source. The additional broadening is evident from the absorption spectrum linewidths, which are 13 MHz at 530°C, but only 11.5 MHz [Fig. 3(a)] at 450°C and lower temperatures. The measured width of 11.5 MHz agrees with the calculated value based on the known natural width of 10 MHz and Doppler broadening due to beam geometry.

#### MEASUREMENT OF THE SPECTRUM

To record the on-resonance spectrum, the frequency of the pump beam and consequently that of the signal beam are locked to the  $(F=2)-(F'=3)$  transition by a feedback loop as shown in Fig. 4 (A/O removed), while the Fabry-Perot interferometer is scanned at a rate of 100 MHz/min. The Fabry-Perot interferometer drift is less than 1 MHz/min. Figure 6(e) is the on-resonance spectrum taken with a peak intensity of 640 mW/cm<sup>2</sup> ( $\pm 10\%$ ) and a sodium oven temperature of 530°C.

For off-resonance spectra, the acousto-optic shifter is placed in the signal beam as shown in Fig. 4, and the laser frequency is stabilized such that the pump-beam frequency is resonant with the  $(F=2)-(F'=3)$  transition; thus the signal beam is held at an accurately known detuning from resonance. The detuning is equal to the oscillator frequency ( $\Delta\nu$ ) applied to the acousto-optic crystal.<sup>28</sup> Figures 6(d) and 6(f) are off-resonance spectra taken under the same conditions as Figure 6(e), but with detunings of -50 and +50 MHz.

The on-resonance spectrum was also measured with a lower sodium temperature to reduce Doppler broadening. Figure 7 is an average of four scans taken with an oven temperature of 450°C and peak laser intensity of 830 mW/cm<sup>2</sup> ( $\pm 10\%$ ).

In addition, the weak-field on-resonance spectrum was observed at both high (530°C) and low (450°C) oven temperatures. The spectra were single lines, with widths of 9.5 and 6 MHz,<sup>21</sup> respectively. These lines theoretically have zero width, and thus are a good measure of the resolution and instrumental line shape of the apparatus.

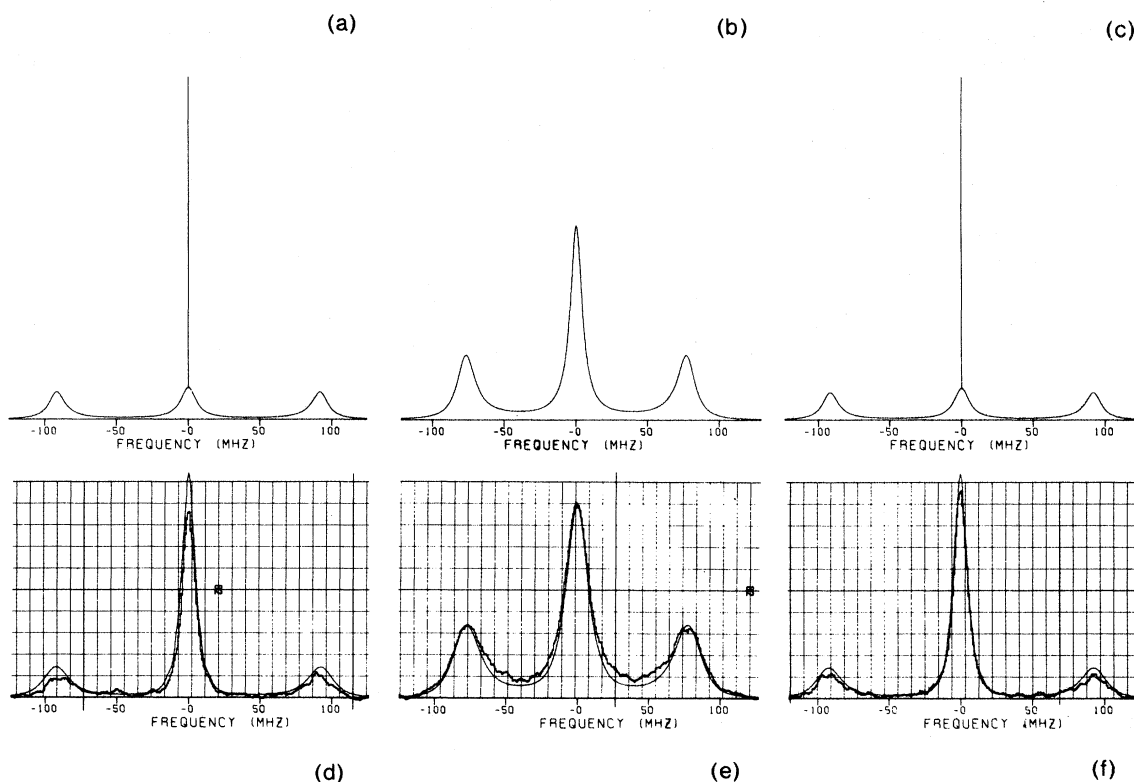


FIG. 6. Theoretical spectra with  $\Omega = 78$  MHz,  $\Gamma = 10$  MHz, and detuning  $\Delta\nu$ . (a)  $\Delta\nu = -50$  MHz, (b)  $\Delta\nu = 0$ , (c)  $\Delta\nu = +50$  MHz. Experimental spectra and convolutions (smooth curve) of theoretical spectra with instrumental line shape. (d)  $\Delta\nu = -50$  MHz, (e)  $\Delta\nu = 0$ , (f)  $\Delta\nu = +50$  MHz. Peak laser intensity  $640$  mW/cm<sup>2</sup>; oven temperature  $530$  °C; vertical scale 35 counts/large division; scan rate 100 MHz/min.

#### DISCUSSION

The curves of Figs. 6(a)–6(c) are plots of the theoretical spectrum [Eq. (1)] corresponding to the data of Figs. 6(d)–6(f). The vertical lines in Figs. 6(a) and 6(c) represent the elastic scattering  $\delta$  function, whose area in this case is 0.46 times the total area of the spectrum. The  $\delta$  function is omitted in Fig. 6(b) because the elastic scattering in the on-resonance spectrum is negligible at this field strength.

For a comparison of theory with experiment, we computed the convolution of the theoretical spectra of Figs. 6(a)–6(c) with the 9.5-MHz-wide instrument line shape of our setup. The convolved spectra are plotted as the smooth curves in Figs. 6(d)–6(f); the vertical scale, which is identical for all three plots, was chosen to make the height of the central peak of the on-resonance convolved spectrum equal to that of the experimental one.

In the on-resonance case, the agreement is very good. The widths of the central and side peaks are 18.8 and 27.3 MHz in the experimental curves and 18.3 and 24.6 MHz in the convolution. The slight nonuniformity of the laser field may account for

the excess width of the side peaks.

For  $\Delta\nu = +50$  MHz, the measured Rabi frequency is very close to that of the convolved spectrum:  $\Omega' = [\Omega^2 + (\Delta\nu)^2]^{1/2} = 92.5$  MHz. The widths of the central and side peaks are 11.3 and 19.7 MHz in the data and 11.0 and 21.5 MHz in the convolved

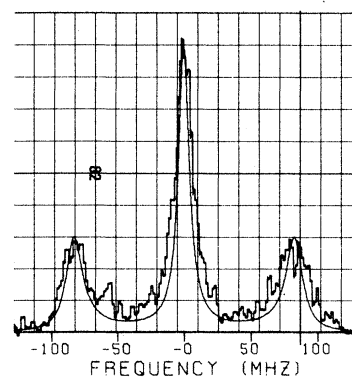


FIG. 7. On-resonance fluorescence spectrum. Vertical scale 5 counts/div. Peak laser intensity  $830$  mW/cm<sup>2</sup>; oven temperature  $450$  °C; scan rate 100 MHz/min. Theoretical spectrum shown as smooth curve.

spectrum, and are clearly narrower than in the on-resonance spectrum. The ratios of the peak heights in the measured and convolved spectra are in good agreement, indicating that the fraction of elastic scattering has increased by the predicted amount.

In the case of  $\Delta\nu = -50$  MHz, the agreement is not as good; the total fluorescence is somewhat less than expected. The decrease of fluorescence may be attributed to the imperfect  $\sigma^+$  circular polarization of the pump and signal beams. At this value of detuning a small component of  $\sigma^-$  polarized light in the signal beam would optically pump some  $F=2$  ( $m_F=2$ ) atoms into the  $F=1$  ground state via the nearly resonant  $F'=2$  excited state.

With our knowledge of the experimental resolution and the theoretical prediction<sup>5</sup> that one-half the fluorescence is in the central peak (in the strong-field limit), we can calculate the number of photons to be expected and compare it with the observed signal. Our calculation shows that in the high-temperature on-resonance spectrum [Fig. 6(e)]  $6 \times 10^4$  photons/sec would be transmitted at the middle of the central peak. Allowing for optical losses in the windows and the interferometer, and 10% quantum efficiency of the photomultiplier, we expect about 600 photoelectron counts/sec. This rough estimate is in reasonable agreement with the measured peak signal of 300

counts/sec.

In the low-temperature spectrum of Fig. 7, the measured widths of the central and side peaks are about 14 and 19 MHz, respectively, and the side peaks are  $82 \pm 2$  MHz from the central peak.<sup>29</sup> The spectrum shows a substantial reduction in the widths of all three peaks as compared with Fig. 6, consistent with the previously mentioned reduction in Doppler broadening. It is compared directly with the exact theory, plotted as the smooth curve in Fig. 7 for  $\Omega = 82$  MHz.<sup>30</sup> The fit is reasonably good, considering that the remaining Doppler broadening and field inhomogeneity have not been included. The poor signal-to-noise ratio in the data is due to the small signal of only 45 counts/sec at the central peak of the spectrum.

#### OBSERVATION OF ASYMMETRIC SPECTRA

Most of the spectra from earlier experiments<sup>19-22</sup> showed some degree of asymmetry. In general, the low-frequency peak was smaller and broader than the high-frequency peak. Theoretical treatments of the two-level atom problem do not account for this effect, but the multilevel-atom calculations of Hopf and Milonni<sup>31</sup> do indicate some asymmetry.

In his most recent experiment, Walther<sup>22</sup> found that the asymmetry depended on the polarization

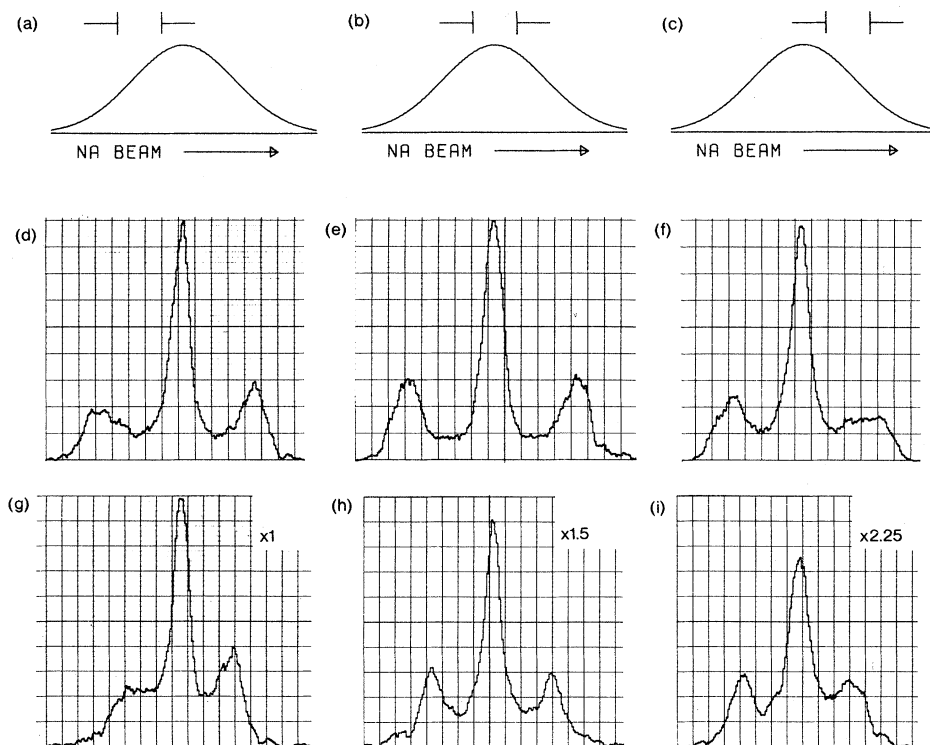


FIG. 8. On-resonance spectra from atoms in a nonuniform field. Laser-beam intensity profile (a) displaced  $-0.5$  mm, (b) centered, (c) displaced  $+0.5$  mm with respect to lower aperture. Under these conditions, spectra (d)–(f) were obtained with  $\sigma^+$  laser light, and (g)–(i) with  $\pi$  laser light. Peak laser intensity  $720$  mW/cm<sup>2</sup>.

of the laser light. The asymmetry of the observed on-resonance spectra was strong with linearly polarized light but very slight with circularly polarized light.

In our experiments we found no asymmetry when the signal beam was centered directly under the observation apertures<sup>32</sup> [Fig. 8(b)], whether the polarization was circular [8(e)] or linear [8(h)]. However, asymmetry was observed when the laser beam was translated 0.5 mm along the atomic beam [Fig. 8(a)]. Figures 8(d) and 8(g), corresponding to  $\sigma^+$  and  $\pi$  excitation, respectively, closely resemble the previously described asymmetric spectra.<sup>19,20,22</sup> When the signal beam was translated 0.5 mm in the opposite direction [Figs. 8(c), 8(f), and 8(i)], we noticed that the asymmetry reversed; i.e., the high-frequency peak was smaller than the low-frequency one.

In the spectrum obtained with  $\pi$  polarization [Fig. 8(h)], the Rabi frequency is less than that obtained with  $\sigma^+$  polarization by the expected amount because of the smaller effective  $|\mu|$  for

$\Delta m = 0$  transitions. In addition, the total fluorescence is less in Figs. 8(h) and 8(i) than in Fig. 8(g) because of optical pumping from the  $F = 2$  to the  $F = 1$  ground state via the nonresonant ( $F = 2$ )-( $F' = 2$ ) transition. [Note that the curves of Figs. 8(g)–8(i) have different vertical scales.]

The data of Figs. 8(d)–8(i) may help resolve the conflict regarding the symmetry of the spectrum reported in earlier experiments.<sup>19–22</sup> It appears that if a substantial amount of fluorescence is collected simultaneously from regions of increasing as well as decreasing laser intensity, an asymmetric spectrum would be obtained with  $\pi$  excitation<sup>19,20</sup> and a symmetric spectrum with  $\sigma^+$  excitation.<sup>22</sup>

At present we are unable to explain the effect, but a more thorough study is being conducted. We believe that it is not an artifact created by misalignment of the apparatus. In any event, it is clear that the polarization of the incident radiation is not a major factor influencing the symmetry of the spectrum.<sup>22</sup>

\*Work supported by the Joint Services Electronics Program.

<sup>1</sup>S. G. Rautian and I. I. Sobel'man, Zh. Eksp. Teor. Fiz. 41, 456 (1961) [Sov. Phys.-JETP 14, 328 (1962)].

<sup>2</sup>P. A. Apanesevich, Opt. Spektrosk. 16, 709 (1964) [Opt. Spectrosc. 16, 387 (1964)].

<sup>3</sup>M. C. Newstein, Phys. Rev. 167, 89 (1968).

<sup>4</sup>V. A. Morozov, Opt. Spektrosk. 26, 116 (1969) [Opt. Spectrosc. 26, 62 (1969)].

<sup>5</sup>B. R. Mollow, Phys. Rev. 188, 1969 (1969).

<sup>6</sup>M. L. Ter-Mikaelyan and A. O. Melikyan, Zh. Eksp. Teor. Fiz. 58, 281 (1970) [Sov. Phys.-JETP 31, 153 (1970)].

<sup>7</sup>C. R. Stroud, Jr., Phys. Rev. A 3, 1044 (1971); *Coherence and Quantum Optics*, edited by L. Mandel and E. Wolf (Plenum, New York, 1973), p.537.

<sup>8</sup>G. Oliver, E. Ressayre, and A. Tallet, Lett. Nuovo Cimento 2, 777 (1971).

<sup>9</sup>R. Gush and H. P. Gush, Phys. Rev. A 6, 129 (1972).

<sup>10</sup>E. V. Baklanov, Zh. Eksp. Teor. Fiz. 65, 2203 (1973) [Sov. Phys.-JETP 38, 1100 (1974)].

<sup>11</sup>G. S. Agarwal, *Quantum Optics* (Springer, New York, 1974), p. 108.

<sup>12</sup>M. E. Smithers and H. S. Freedhoff, J. Phys. B 7, L432 (1974); 8, L209 (1975).

<sup>13</sup>H. J. Carmichael and D. F. Walls, J. Phys. B 8, L77 (1975).

<sup>14</sup>S. S. Hassan and R. K. Bullough, J. Phys. B 8, L147 (1975).

<sup>15</sup>C. Cohen-Tannoudji, in *Proceedings of the Second Laser Spectroscopy Conference, Megève, France, 1975* (Springer, Berlin, 1975).

<sup>16</sup>S. Swain, J. Phys. B 8, L437 (1975).

<sup>17</sup>B. R. Mollow, Phys. Rev. A 12, 1919 (1975).

<sup>18</sup>H. J. Kimble and L. Mandel, Phys. Rev. Lett. 34, 1485 (1975); Opt. Commun. 14, 167 (1975); Phys. Rev. A 13, 2123 (1976).

<sup>19</sup>F. Schuda, C. R. Stroud, Jr., and M. Hercher, J. Phys. B 7, L198 (1974).

<sup>20</sup>H. Walther, in Ref. 15.

<sup>21</sup>F. Y. Wu, R. E. Grove, and S. Ezekiel, Phys. Rev. Lett. 35, 1426 (1975).

<sup>22</sup>H. Walther, Paper IA4, Seventh Annual Meeting of the Division of Electron and Atomic Physics, American Physical Society, Tucson, Arizona, 1975 (unpublished).

<sup>23</sup>V. Weisskopf, Ann. Phys. Leipzig 9, 23 (1931).

<sup>24</sup>H. M. Gibbs and T. N. C. Venkatesan, Opt. Commun 17, 87 (1976).

<sup>25</sup>P. Eisenberger, P. M. Platzman, and H. Winick, Phys. Rev. Lett. 36, 623 (1976).

<sup>26</sup>J. A. Abate, Opt. Commun. 10, 269 (1974).

<sup>27</sup>F. Y. Wu, R. E. Grove, and S. Ezekiel, Appl. Phys. Lett. 25, 73 (1974); R. E. Grove, F. Y. Wu and S. Ezekiel, Opt. Eng. 13, 531 (1974).

<sup>28</sup>In practice the A/O shifter was placed in the pump beam so that the critical alignment of the signal beam was not affected by detuning. The pump beam was realigned to compensate for the angular deflection of the A/O shifter.

<sup>29</sup>Calculation of the Rabi frequency from the measured intensity gives  $83 \pm 4$  MHz, in good agreement with observation.

<sup>30</sup>For  $\Omega = 82$  MHz the width of the central peak of the theoretical spectrum is 10.2 MHz and the width of the side peaks is 15.4 MHz.

<sup>31</sup>F. A. Hopf and P. W. Milonni, Paper AB8, in Ref. 22.

<sup>32</sup>This position was determined by translating the laser beam to obtain the largest Rabi frequency.